THE JOURNAL OF COMPARATIVE NEUROLOGY 505:177–189 (2007)

Displaced Amacrine Cells of the Mouse Retina

LUIS PÉREZ DE SEVILLA MÜLLER, JENNIFER SHELLEY, AND RETO WEILER*
Department of Neurobiology, University of Oldenburg, D-26111 Oldenburg, Germany

ABSTRACT

The aim of this study was to characterize and classify the displaced amacrine cells in the mouse retina. Amacrine cells in the ganglion cell layer were injected with fluorescent dyes in flat-mounted retinas. Dye-filled displaced amacrine cells were classified according to dendritic field size, horizontal and vertical stratification patterns, and general morphology. We identified 10 different morphological types of displaced amacrine cell. Six of the cell types identified here are novel cell types that have not been described previously in the mouse retina, to the best of our knowledge. The displaced amacrine cells included four types of medium-field cells, with dendritic field diameters of 200–500 μm, and six types of wide-field cells, with dendritic fields extending over 500 μm. Narrow-field displaced amacrine cells, with dendritic field diameters smaller than 200 μm, were not encountered. The most frequently labeled displaced amacrine cell type was the starburst amacrine cell. At least three cell types identified here have nondisplaced counterparts in the inner nuclear layer as well. Displaced amacrine cells display a rich variety of stratification and branching patterns, which surely reflect the wide range of their functional roles in the processing of visual signals in the inner retina. J. Comp. Neurol. 505:177–189, 2007.

Indexing terms: retina; displaced amacrine cell; mouse; morphology; dye injection

Amacrine cells play an important role in processing of visual information in the inner retina. These neurons make inhibitory synapses onto bipolar and ganglion cells in the inner plexiform layer (IPL), modulating the spatial and temporal properties of the visual signals passed from bipolar cells to ganglion cells. Amacrine cells vary widely in morphology and function (Massey and Redburn, 1987; Vaney, 1990; Strettoi and Masland, 1996; Masland, 2001) and can have complex neurochemical signatures, expressing either GABA or glycine, along with acetylcholine or other neuropeptides (Marc et al., 1995). The main division into GABAergic and glycinergic cells is often correlated with dendritic field size (Vaney, 1990; Wässle and Boycott, 1991).

The cell bodies of amacrine cells can be located in the inner nuclear layer (INL) or in the ganglion cell layer (GCL): amacrine cells located in the GCL are termed *displaced amacrine cells*. Displaced amacrine cells can easily be distinguished from ganglion cells by their small soma and their lack of an axon that projects to the brain. The first evidence that the small cells in the GCL are neurons and not glia cells was presented by Hughes and Wieniawa-Narkiewicz (1980) for the cat retina. Since then, the morphology and branching patterns of displaced amacrine cell types have begun to be examined: six types of displaced amacrine cell have been identified in the rat retina (Perry and Walker, 1980), 11 types in the guinea pig (Kao and Sterling, 2006), and four types in the cat retina (Wässle et al., 1987a).

So far, 11 types of displaced amacrine cell have been identified in the mouse retina (Gustincich et al., 1997; Badea and Nathans, 2004; Lin and Masland, 2006). However, most of these cell types were identified by using transgenic approaches, which may not reveal every cell type that is present in wild-type mice. Displaced amacrine cells make up about 59% of the somata within the mouse GCL (Jeon et al., 1998); because 20–40 different types of amacrine cell are thought to exist in the vertebrate retina (Massey and Redburn, 1987; Vaney, 1990; Strettoi and Masland, 1996; Masland, 2001), it is likely that many displaced amacrine cell types have been overlooked. With the growing prominence of transgenic mice in retinal re-

Grant sponsor: Deutsche Forschungsgemeinschaft.

*Correspondence to: Dr. Reto Weiler, Department of Neurobiology, University of Oldenburg, P.O. Box 2503, D-26111 Oldenburg, Germany. E-mail: reto.weiler@uni-oldenburg.de

Received 6 February 2007; Revised 12 July 2007; Accepted 1 August 2007

DOI 10.1002/cne.21487

Published online in Wiley InterScience (www.interscience.wiley.com).

search, a better understanding of mouse retinal architecture is essential.

The aim of this study was to characterize and classify the displaced amacrine cells in the mouse retina. A wide range of techniques is available for visualizing retinal neurons. To identify as many cells as possible, we combined two approaches: 1) random dye injection of amacrine cells in the GCL of wild-type retinas and 2) targeted dye injection of amacrine cells in the GCL of transgenic mice in which distinct populations of cells are labeled with green fluorescent protein (EGFP). Displaced amacrine cells were then classified according to their dendritic field size, horizontal and vertical branching patterns, and general morphology. The stratification depth of the amacrine cell processes within the IPL was determined by immunohistochemical labeling of the two plexi of cholinergic starburst amacrine cells, which visually define the five layers of the IPL.

We identified 10 different types of displaced amacrine cell. Four of these cell types were characterized as medium-field, since their dendritic fields had diameters of 200–500 μm. Among the four medium-field amacrine cell types, three types were monostratified, including the starburst amacrine cell, and one type was bistratified. The remaining six displaced amacrine cell types were defined as wide-field, with dendritic fields extending over 500 μm. Wide-field amacrine cells included five types of monostratified and one type of multistratified cell. Four displaced amacrine cell types identified in this study closely resemble amacrine cells described previously for other mammalian retinas (Perry and Walker, 1980; Vaney et al., 1981; Kolb et al., 1981; Wässle et al., 1987a,b; Famiglietti 1992b), indicating common functional roles. Six of the cell types identified here are novel cell types that have not been described previously in the mouse retina. In addition to these six cell types, 11 displaced amacrine cell types have been described previously in studies using transgenic mouse models (Gustincich et al., 1997; Badea and Nathans, 2004; Lin and Masland, 2006). Thus, different methods appear to reveal different cell types selectively, and the present catalog of 17 displaced amacrine cells types might not yet be complete. Nevertheless, this study provides a basic anatomical reference for future functional studies of displaced amacrine cells in the mouse retina.

MATERIALS AND METHODS

Preparation

Animals were handled in accordance with institutional guidelines for animal welfare. Adult C57/Bl6 and Cx45-EGFP (Maxeiner et al., 2005) mice were killed by cervical dislocation. Retinas were removed and mounted photoreceptor side down on black filter paper (Millipore Corporation, Bedford, MA). Retinas were then incubated at room temperature in mouse Ringer, which contained (in mM): 137 NaCl, 5.4 KCl, 1.8 $CaCl_2 \cdot 2\ H_2O$, 1 $MgCl_2 \cdot 6\ H_2O$, 5 HEPES, and 10 glucose, adjusted to pH 7.4 with 0.1 N NaOH.

Intracellular injections

The methods for intracellular injections have been described previously (Schubert et al., 2005). Briefly, borosilicate glass electrodes (Hilgenberg GmbH, Malsfeld, Germany) were filled with 4% N-(2-aminoethyl-)-biotinamide hydrochloride (Neurobiotin; Vector Laboratories, Burlingame, CA) and either 0.5% Lucifer yellow (Sigma, St. Louis, MO) or Alexa Fluor 594 (Molecular Probes, Eugene, OR) dissolved in Tris buffer (pH 7.4–7.5), with typical resistances between 170 and 300 MΩ. For random injection of displaced amacrine cells in wild-type retinas, cell bodies in the GCL were visualized with acridine orange (1 μM; Sigma, St. Louis, MO) under a ×40 water-immersion objective. For targeted injection in Cx45-EGFP retinas, the EGFP signal was used to target amacrine cells in the GCL. Lucifer yellow or Alexa Fluor 594 was iontophoresed with negative current of 1 nA (750 msec at 1 Hz); as soon as the dendritic morphology of the cell became visible, the direction of the current was reversed to inject positively charged Neurobiotin molecules. After the final injection, which lasted for 2–3 minutes, the retina remained for at least 30 minutes in the recording chamber, allowing diffusion of Neurobiotin. Retinas were then fixed in 4% paraformaldehyde for 10 minutes and washed for at least 30 minutes in 0.1 M phosphate buffer (PB), pH 7.4. Neurobiotin was visualized by incubating injected retinas overnight with streptavidin-indocarbocyanine (Cy3; Jackson Immunoresearch, West Grove, PA; dilution 1:500), in 0.1 M PB containing 0.3% Triton X-100 (Sigma). Retinas were mounted in Vectashield (Vector Laboratories, Burlingame, CA) and stored in the dark at 4°C.

Immunohistochemistry and confocal microscopy

After cell injection and fixation, retinas were labeled with polyclonal goat antibodies raised against human placental choline acetyltransferase (ChAT; 1:100; No. AB144P; Chemicon International, Temecula, CA). The antiserum stains a single band of 68–70 kD molecular weight in Western blot (manufacturer's technical information). Anti-ChAT antibodies label the dendritic processes of starburst amacrine cells in layers S2 and S4 of the IPL (Haverkamp and Wässle, 2000; Schubert et al., 2005), allowing visualization of the ON and OFF sublaminae of the IPL. In addition, rabbit anti-γaminobutyric acid (GABA; 1:100; raised in rabbit against GABA coupled to porcine thyroglobin; kindly donated by D. Pow, University of Newcastle, Australia; Pow et al., 1995) and rat antiglycine antibodies (1:1,000; raised in rat against glycine coupled to porcine thyroglobin; kindly donated by D. Pow; Pow et al., 1995) were used to determine the neurotransmitter expression of amacrine cells in the GCL. Specificity of the GABA and glycine antibodies was tested previously and has been explained in detail by Pow et al. (1995). Briefly, specificity was tested by using immunoblotting against the same amino acid-paraformaldehyde-thyroglobulin conjugates used to immunize the animals: both antibodies labeled blots containing conjugates of the appropriate amino acid (Pow et al., 1995). All antibodies employed in this study have been used previously on paraformaldehyde-fixed tissue; our results are identical to those previously reported (Haverkamp and Wässle, 2000; Schubert et al., 2005).

Retinas were blocked with donkey serum diluted 1:15 in PB with 0.3% Triton X-100 and incubated overnight at 4°C. Retinas were then incubated for 1 week in primary antibodies (diluted as noted in PB with 0.1% NaN_3), washed several times in PB, and incubated overnight at 4°C in the corresponding secondary antibodies: donkey anti-goat Cy3 (1:500; Jackson Immunoresearch; catalog

TABLE 1. Overview of the Classification of the Displaced Amacrine Cells

	Medium-field				*Wide-field*					
Cell type	MA-S1	Starburst	MA-S5	MA-S1/S5	WA-S1	WA-S3	A17	PA-S1	PA-S5	Multi-stratified
Soma diameter	7.5 ± 1.2	8.3 ± 1.8	7.7 ± 0.8	7.1	7.8 ± 0.5	8.0 ± 0.8	11.8 ± 0.7	12.0 ± 0.2	9.5 ± 0.5	10.0 ± 1.7
Dendritic field diameter	219 ± 21	279 ± 39	350 ± 2	283	1250 ± 560	1510 ± 850	878 ± 285	737 ± 122	1072 ± 220	2210 ± 240
Cells injected	4	87	6	1	12	4	4	2	8	3

No. 705-095-003), goat anti-rat Cy3 (1:500; Dianova, Karlsruhe, Germany; catalog No. 81-9515), or donkey anti-rabbit Cy3 (1:500; Jackson Immunoresearch; catalog No. 711-165-152). Retinas were then washed in PB and mounted in Vectashield. Images were taken with a Leica TCS SL confocal microscope with a ×40 oil-immersion objective. Intensity and contrast of the final images were adjusted in Adobe Photoshop 7.0.

RESULTS

Morphological classification of displaced amacrine cell types

To characterize and classify mouse displaced amacrine cells, we injected amacrine cells in the GCL with Lucifer yellow and Neurobiotin. Dendritic stratification was determined by labeling with anti-ChAT antibodies, which visually define the five strata of the IPL. Over 400 displaced amacrine cells were filled in the course of this study. Among these, 131 met the criterion of complete labeling, established by the appearance of terminal dendritic tips, and were used for analysis. We created a morphological catalog of the injected displaced amacrine cells by using three primary parameters: 1) dendritic field size, 2) depth of stratification in the IPL, and 3) branching pattern of the dendrites. With these criteria, we identified 10 types of displaced amacrine cell in the mouse retina. Nine of these cell types were found in the wild-type retina, whereas one type, the A17 cell, was so rare that it was encountered only with targeted injection of EGFP-labeled neurons in a transgenic mouse line. In general, the size and depth of stratification of the dendritic arbor were sufficient to separate cells into distinct types.

Table 1 gives an overview of the classification of the displaced amacrine cells identified in this study. Displaced amacrine cells were divided into two groups according to their dendritic field size: medium-field cells, with dendritic field diameters ranging from 200 to 500 μm, and wide-field cells, with dendritic fields larger than 500 μm. Most amacrine cells injected in the GCL had round or oblong dendritic fields, although some wide-field amacrine cells with asymmetric dendritic fields were observed. With the exception of the A17 cell and one type of polyaxonal amacrine cell, the somata of the displaced amacrine cells were small, ranging in diameter from 7 to 10 μm. Novel cell types were named according to the IPL strata in which their dendrites branched.

Medium-field displaced amacrine cells

Cells with dendritic field diameters of 200–500 μm were defined as medium-field amacrine cells (MA). These cells were divided into four types based on stratification depth within the IPL (Fig. 1). Three of these cell types, including the starburst amacrine cell, were monostratified, and one type was bistratified.

MA-S1 cells made up 3% of the displaced amacrine cells encountered in this study. A typical cell of this type can be seen in Figure 1b. The dendritic arborization of this cell is approximately 220 μm across and has an asymmetric, though dense and space-filling branching pattern. The dendrites of this cell type stratify in layer S1 of the IPL (Fig. 1a,c) and do not have dendritic spines. The round cell body is small, averaging 7.5 ± 1.2 μm in diameter (n = 4). The distinctive morphology of these neurons was consistent from cell to cell.

Starburst amacrine cells are found in every vertebrate class and are easily recognized by their distinctive morphology (for review see Masland and Tauchi, 1986). These highly symmetrical cells have six or more primary dendrites that project radially from the soma, branching progressively with distance from the soma (Fig. 1e). Starburst cells have round or ovoid dendritic arbors of 279 ± 39 μm diameter (n = 87), which stratify in layer S4 of the IPL (Fig. 1d,f). The cell body has a mean diameter of 8.3 ± 1.8 μm. We found starburst amacrine cells to be the predominant amacrine cell type in the GCL; 66% of the cells injected in this study were starburst amacrine cells. Displaced starburst cells are ON cells, and their OFF counterparts have cell bodies located in the INL and stratify in layer S2.

Monostratified MA-S5 cells made up approximately 5% of the cells injected in this study. An example of this cell type is illustrated in Figure 1h. The MA-S5 cell has a disorganized, asymmetric dendritic field of 350 ± 2 μm diameter (n = 6), which ramifies in layer S5 of the IPL (Fig. 1g,i). Most of the dendrites occupy the same semicircle of space and arise from two to three primary dendrites. These primary dendrites protrude from opposite sides of the cell body and are quite long, although their branches are short and sparse. The dendrites of these cells are covered in prominent varicosities. MA-S5 cell somata have diameters of 7.7 ± 0.8 μm.

The MA-S1/S5 cell was the only type of bistratified amacrine cell that we found in the GCL. This cell type appears to be exceptionally rare: we encountered only one MA-S1/S5 cell in the course of this study. The morphology of this cell type can be seen in Figures 1k and 2. This cell has two narrowly stratified, asymmetric dendritic arbors located in layers S1 and S5 of the IPL (Fig. 1j,l, 2). The dendritic field of this cell extends approximately 283 μm and has a dense and chaotic branching pattern. The dendritic branches in the ON and OFF layers are shown separately in Figure 2.

Wide-field displaced amacrine cells

Wide-field amacrine cells (WA) have dendritic fields larger than 500 μm (Kolb, 1982; Masland, 1988). We identified six types of displaced WA, classified according to their stratification patterns in the IPL. Five of these cell types were monostratified, including two types of polyax-

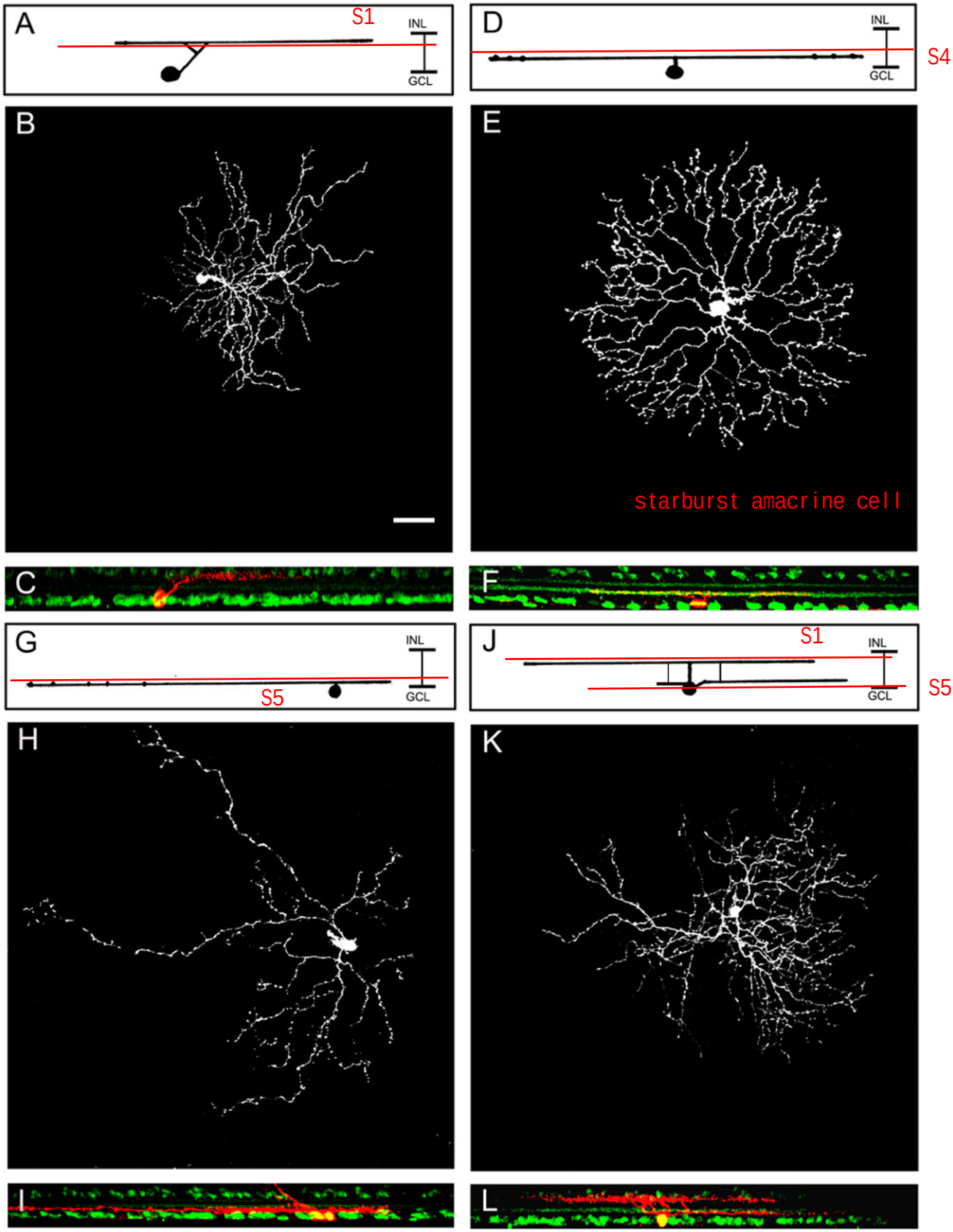
A
S1
INL
GCL
D
INL
GCL
S4
B
E
starburst amacrine cell
C
F
G
INL
S5
GCL
J
S1
INL
GCL
S5
H
K
I
L

Figure 1

onal amacrine cell, and one type was multistratified (Fig. 3).

The WA-S1 has a distinctive bow tie shape, with three to five unbranched dendrites projecting from either side of its round soma (Fig. 3b). The dendrites are long and straight, covering a distance of up to 1 mm, and stratify in layer S1 of the IPL (Fig. 3a,c). These cells have a soma diameter of 7.8 ± 0.5 μm (n = 12). The WA-S1 cell has been described previously from other species (Gallego, 1971; Perry and Walker, 1980; Wässle et al., 1987b). As with starburst amacrine cells, WA-S1 cells also have non-displaced counterparts in the INL (Perry and Walker, 1980; Wässle et al., 1987b; MacNeil and Masland, 1998).

The WA-S3 was the second type of monostratified wide-field amacrine cell identified in this study. An example of this cell type can be seen in Figure 3e. This cell has a round dendritic field, which stratifies in layer S3 of the IPL (Fig. 3d,f). The dendrites of this amacrine cell are largely unbranched and project radially from the cell body, extending for 1.51 ± 0.85 mm. Prominent varicosities are present on the entire length of the dendrites.

In the Cx45-EGFP mouse retina, distinct populations of cells are labeled with EGFP (Maxeiner et al., 2005). We injected somata in the GCL of these retinas and found that the EGFP-positive amacrine cells were displaced A17 cells. One such cell can be seen in Figure 3h. This cell has a dense dendritic field, which stratifies in layer S5 of the IPL (Fig. 3g,i). The dendrites of this cell extend radially from the cell body and are covered in prominent varicosities. Because of their low density, these highly conserved cells were not encountered in the wild-type retina (see Discussion).

We found only one type of multistratified WA in the GCL. A prominent characteristic of this cell is its kinky dendrites, which make several sharp turns before ending approximately 2 mm from the soma (Fig. 3k). The dendrites of this cell do not fill out the region of arborization; branching is infrequent but dramatic, often at angles larger than 90°. This cell has some long dendrites that stratify in layer S5 of the IPL, whereas shorter dendrites extend into layers S1, S2, and S3 (Fig. 3j,l). The soma of this cell is small and round, with a diameter of 10 ± 1.7 μm (n = 3).

Polyaxonal (PA) amacrine cells have between one and six branching, axon-like processes that project from the cell body or from the dendrites near the cell body. These fine processes maintain a uniform thickness and branch dramatically at right angles (Famiglietti, 1992a,b). Six physiologically distinct PA amacrine cells have been identified in the rabbit retina (Völgyi et al., 2001), and several morphological types exist in the mouse retina as well (Lin and Masland, 2006).

PA-S1 cells have the largest somata of all displaced amacrine cells identified in this study, with a diameter of 12.0 ± 0.2 μm (n = 2). This cell type has an asymmetric dendritic field with a diameter of approximately 740 μm. The dendrites leave the cell body in layer S5, where the dendrites branch off from the axon-like processes. Both dendrites and axon-like processes terminate in layer S1 (Fig. 4a,c). The thin dendrites of this amacrine cell are sparse and somewhat wavy and display the right-angled branch points described previously (Fig. 4b,d; Famiglietti, 1992a,b).

PA-S5 cells have a few large dendrites, which extend approximately 1 mm and stratify in layer S5 of the IPL (Fig. 4e,g). This amacrine cell has thick and comparatively straight axon-like processes that are decorated with prominent varicosities (Fig. 4f). The dendrites of this cell are sparsely branched and asymmetrical (Fig. 4h). This cell type has a round soma with a diameter of 9.5 ± 0.5 μm (n = 8). The PA-S5 cell is similar to the displaced PA2 cell reported for the rabbit retina (Famiglietti 1981, 1992b).

Neurotransmitter expression

Amacrine cells are the major inhibitory neurons in the mammalian retina, and they can use either GABA or glycine for neurotransmission (for review see Vaney, 1990; Wässle and Boycott, 1991). We used antibodies against GABA and glycine to determine which neurotransmitter is expressed in amacrine cells in the GCL. Antibodies against GABA produced a uniform distribution of labeled somata in the GCL (n = 2; Fig. 5a). Because ganglion cells typically do not express GABA (see, e.g., Watt et al., 1994; Zhang et al., 2004), these GABA-positive cells were probably displaced amacrine cells. Very few cells in the GCL were labeled with antibodies against glycine (n = 3; Fig. 5b). The small number of glycine-immunoreactive cell bodies in the GCL was not a result of technical errors, because numerous cell bodies in the INL were strongly labeled (not shown). This finding suggests that most, if not all, displaced amacrine cells use GABA as their neurotransmitter. Similar findings have been reported in other species (Wässle et al., 1987a; Kao and Sterling, 2006).

DISCUSSION

Displaced amacrine cells make up one-third to two-thirds of all neurons in the GCL (Perry and Walker, 1980; Hughes and Vaney, 1980; Hughes and Wieniawa-Narkiewicz, 1980; Linden and Esbérard, 1987; Abreu et al., 1993; Jeon et al., 1998) and comprise several different cell types (Perry and Walker, 1980; Wässle et al., 1987a; Völgyi et al., 2001; Badea and Nathans, 2004; Kao and Sterling, 2006). Although morphological and electrophysiological studies in some species have made progress to-

Fig. 1. Examples of the branching and stratification patterns of the medium-field displaced amacrine cells in the mouse retina. **A:** Illustration of the stratification of the MA-S1 cell. These rare monostratified medium-field displaced amacrine cells stratify in layer S1 of the inner plexiform layer and have asymmetric, densely branched dendrites. **B:** Confocal image of an MA-S1 cell injected with Neurobiotin, showing the dendritic branching pattern in tangential view. **C:** Confocal image of an MA-S1 cell injected with Neurobiotin (red) and counterstained with ChAT antibodies (green) to indicate stratification depth; this image shows the stratification pattern of the MA-S1 cell in radial view. **D:** Illustration of the stratification of the starburst amacrine cell. These widely conserved medium-field cells are highly symmetrical, with six or more primary dendrites projecting radially from the soma and stratifying in layer S4 of the inner plexiform layer. **E,F:** Confocal image of a starburst amacrine cell in tangential (E) and radial (F) views. **G:** Illustration of the stratification of the MA-S5 cell. These cells have asymmetric dendritic fields, which stratify in layer S5 of the inner plexiform layer. Most of the dendrites carve out an approximate semicircle and branch off from two or three primary dendrites. **H,I:** Confocal image of a MA-S5 cell in tangential (H) and radial (I) views. **J:** Illustration of the stratification of the MA-S1/S5 cell. These bistratified cells have densely branching dendrites that stratify in layers S1 and S5 of the inner plexiform layer. **K,L:** Confocal image of a MA-S1/S5 cell in tangential (K) and radial (L) views. Scale bar = 40 μm.

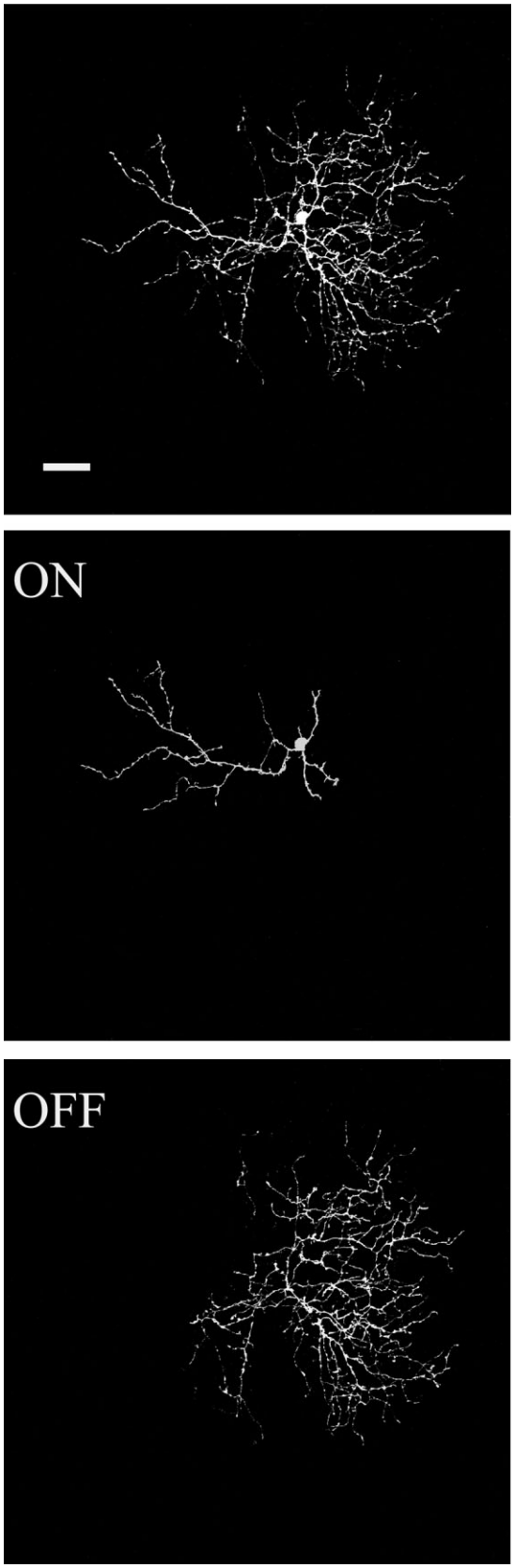

ward understanding the roles of displaced amacrine cells (e.g., Menger and Wässle, 2000; Völgyi et al., 2001; Aboelela and Robinson, 2004), similar efforts in mouse have just begun (Badea and Nathans, 2004; Lin and Masland, 2006). In this study, we identify 10 morphologically distinct types of displaced amacrine cell in the mouse retina, which include medium- and wide-field cells (Fig. 6); six of these cell types have not been described previously for the mouse.

Methodological considerations

Several different cell labeling techniques have been used to examine displaced amacrine cells. Early classification studies applied Golgi staining (turtle: Kolb, 1982; cat: Wässle et al., 1987a; rabbit: Famiglietti 1992a,b); this method labels a small number of neurons in their entirety but provides no quantitative information. More recently, photofilling (MacNeil et al., 1999) and tracer injection (Völgyi et al., 2001) techniques, as well as immunolabeling combined with tracer injection (Kao and Sterling, 2003), have been used to examine displaced amacrine cells. In contrast to the Golgi method, these techniques allow estimation of population size (see MacNeil et al., 1999). In the present study, we combined two approaches to classify displaced amacrine cells in the mouse retina: we randomly injected amacrine cells in the GCL of wild-type retinas, and we methodically injected EGFP-labeled amacrine cells in transgenic mice (connexin45-expressing cells; see Maxeiner et al., 2005). Targeted injection in the EGFP mouse line revealed only one cell type that was not found by random injection in the wild-type retina: the highly conserved A17 cell. Whereas nondisplaced A17 cells form a highly packed mosaic, displaced A17 cells are much less numerous (approximately 3 cells/mm^2: this study, data not shown; Sandell and Masland, 1986); our failure to encounter this cell type in the wild-type retina is probably a reflection of this low cell density.

Fig. 2. Confocal images of a bistratified MA-S1/S5 cell. The upper panel is a stack showing all dendrites in tangential view. The lower two panels show the dendritic arborizations in the ON and OFF layers separately. Scale bar = 40 μm.

Fig. 3. Examples of the branching and stratification patterns of four types of wide-field displaced amacrine cell. **A:** Illustration of the stratification of the WA-S1 cell. These distinctive wide-field cells have long, straight dendrites extending from either side of the cell body and stratifying in layer S1 of the inner plexiform layer. **B:** Confocal image of an WA-S1 cell injected with Neurobiotin, showing the dendritic branching pattern in tangential view. **C:** Confocal image of an WA-S1 cell injected with Neurobiotin (red) and counterstained with ChAT antibodies (green) to indicate stratification depth; this image shows the stratification pattern of the WA-S1 cell in radial view. **D:** Illustration of the stratification of the WA-S3 cell. These wide-field cells have sparsely branched asymmetrical dendrites that ramify in layer S3 of the inner plexiform layer. **E,F:** Confocal image of a WA-S3 cell in tangential (E) and radial (F) views. **G:** Illustration of the stratification of the A17 cell. These cells were found in retinas of Cx45-EGFP mice, in which some neuron populations are labeled with EGFP (Maxeiner et al., 2005). This highly conserved cell stratifies in layer S5 of the inner plexiform layer. **H,I:** Confocal image of a A17 cell in tangential (H) and radial (I) views. **J:** Illustration of the stratification of the multistratified WA cell. These wide-field cells have several long, dramatically branching dendrites, which stratify in layer S5 of the inner plexiform layer, and shorter dendrites, which extend into layers S1, S2, and S3. **K,L:** Confocal image of a multistratified WA cell in tangential (K) and radial (L) views. Scale bar = 40 μm.

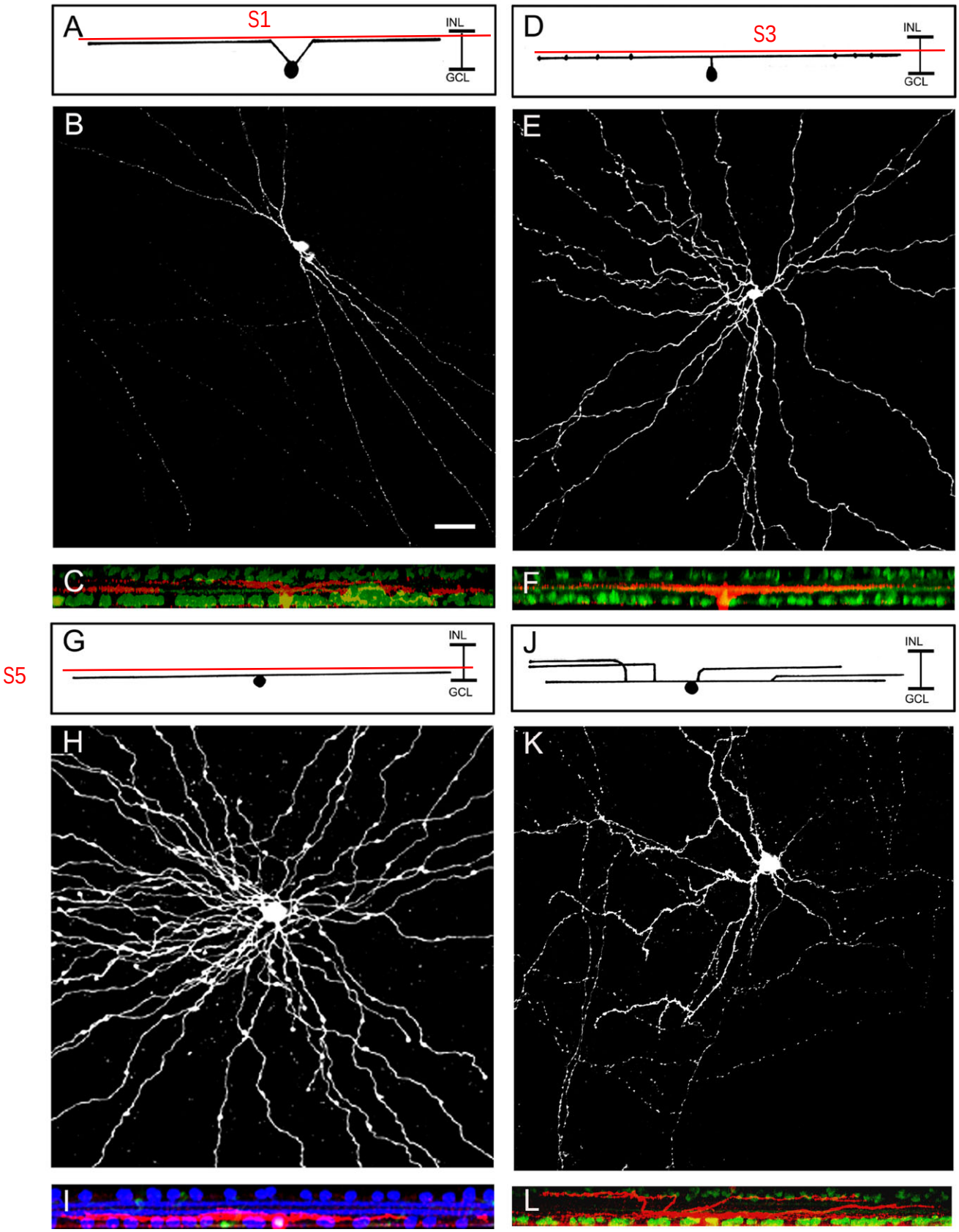

Figure 3

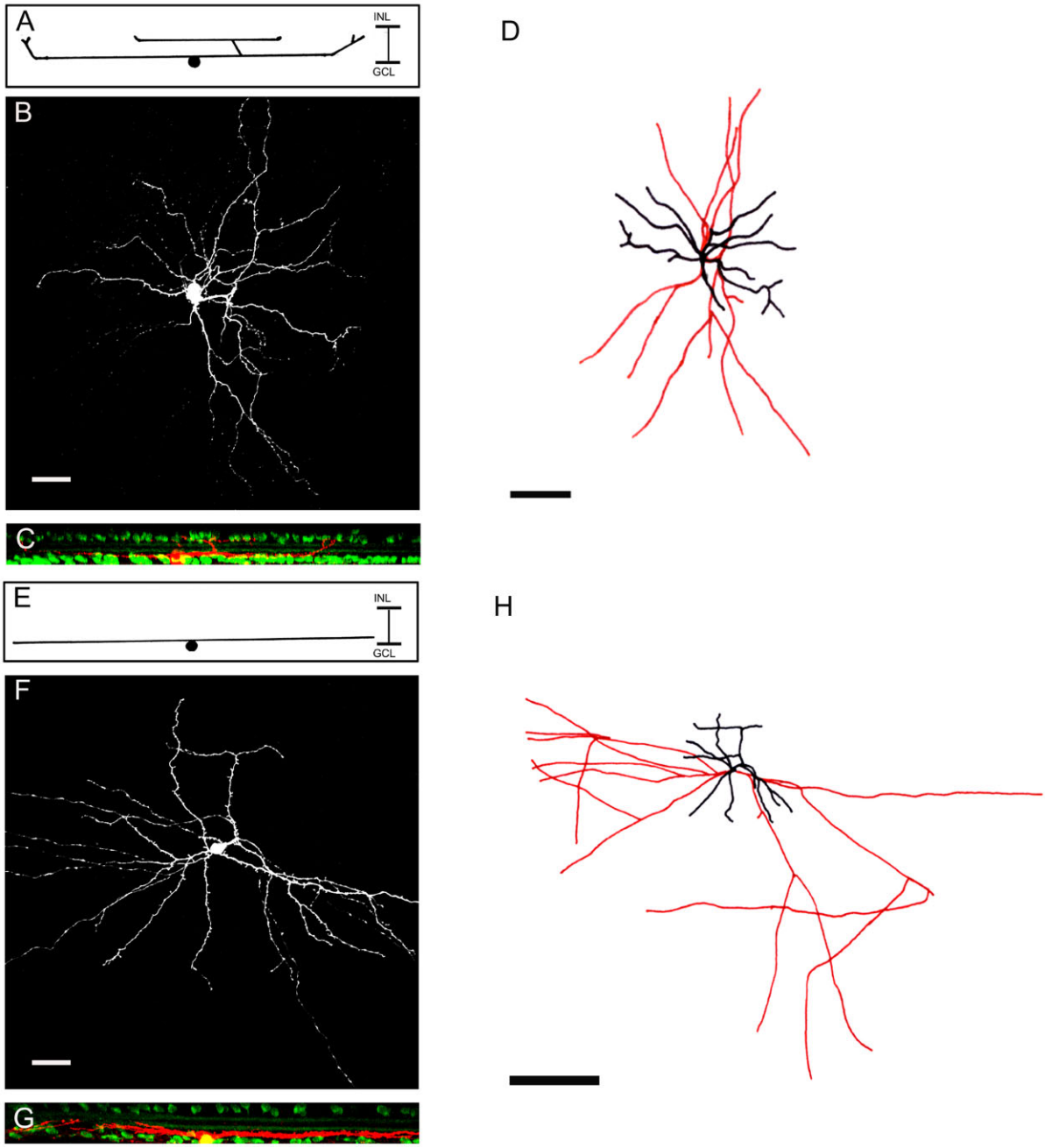

Fig. 4. Examples of the branching and stratification patterns of polyaxonal displaced amacrine cells. **A:** Illustration of the stratification of the PA-S1 cell. These polyaxonal cells have asymmetric dendrites, which leave the cell body in layer S5, where they extend before turning upward and ending in S1 of the inner plexiform layer. **B,C:** Confocal image of a PA-S1 cell in tangential (B) and radial (C) views. **D:** Illustration of the dendritic (black) and axon-like processes (red) of the PA-S1 cell. **E:** Illustration of the stratification of the PA-S5 cell. These polyaxonal cells have sparsely branched, asymmetric dendrites, which stratify in layer S5 of the inner plexiform layer. **F,G:** Confocal image of a PA-S5 cell in tangential (F) and radial (G) views. **H:** Illustration of the dendritic (black) and axon-like processes (red) of the PA-S5 cell. Scale bars = 40 μm in B (applies to B,C); 40 μm in F (applies to F,G); 100 μm in D; 200 μm in H.

How do our results compare with previous studies of displaced amacrine cells in the mouse? Six of the cells identified here have not been described previously in the mouse: MA-S1, MA-S1/S5, WA-S3, PA-S1, displaced A17, and multistratified WA. Starburst amacrine cells have been described extensively in several species, including mouse (see, e.g., Masland and Tauchi, 1986; Menger and Wässle, 2000; Petit-Jacques et al., 2005). The MA-S5 cell may correspond to the displaced cluster 3 cells described by Badea and Nathans (2004). The WA-S1 cell was reported recently by Lin and Masland (2006). Our PA-S5 cell may correspond to the WA4-1 cell of Lin and Masland

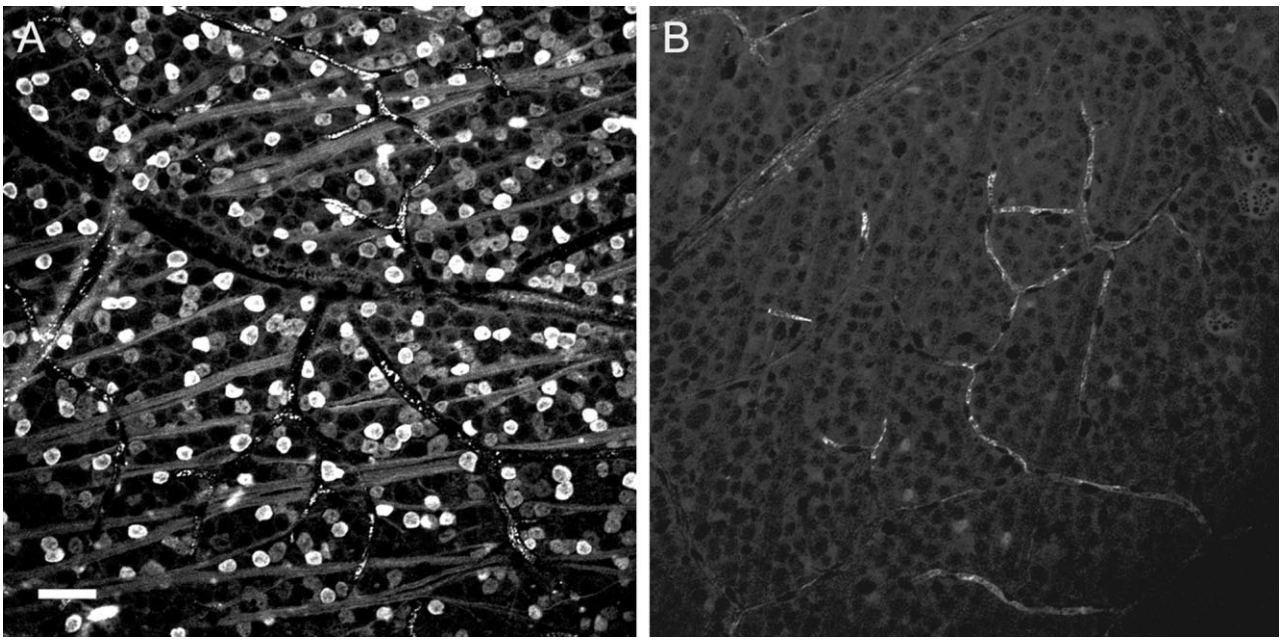

Fig. 5. Neurotransmitter expression in the ganglion cell layer of the mouse retina. **A:** Large numbers of cells are immunoreactive for GABA in the ganglion cell layer; these cells are presumably displaced amacrine cells, because ganglion cells do not show GABA immunoreactivity. In comparison, glycine immunoreactivity is rare in cell bodies in the ganglion cell layer (**B**). Scale bar = 40 μm.

(2006); the morphology is quite similar, although we disagree regarding the cell's stratification. This disagreement could arise from differences in interpretation: Lin and Masland (2006) did not use any marker to label the strata of the IPL and thus could make stratification assignments only "with some confidence"; in addition, we define stratification as the level at which the dendrites terminate, whereas Lin and Masland (2006) might have looked at the average depth over the length of the dendrites, as was done by Badea and Nathans (2004). However, it is also possible that Lin and Masland's (2006) WA4-1 and our PA-S5 cell are two different cell types with similar morphologies.

Six displaced amacrine cell types identified in transgenic mouse strains by Badea and Nathans (2004) were not found in the present study: A1-1, A1-2, cluster 1, cluster 4, bifid, and giant amacrine cells. In addition, Gustincich et al. (1997) reported a displaced catecholaminergic cell in the mouse retina that stratifies in S3. These discrepancies highlight the importance of comparing the results of several methodological approaches when classifying retinal cell types. Neither our dye injection technique nor the transgenic approaches used by Badea and Nathans (2004) and Lin and Masland (2006) can be certain of finding every cell type. When injecting cells, the experimenter may be biased against some cell types. For example, to avoid filling ganglion cells, we injected cells with small cell bodies; therefore, it is possible that we overlooked displaced amacrine cells with large cell bodies. In addition, cells present in low numbers may be missed with this technique. On the other hand, studies using transgenic mouse lines cannot be certain that every type of cell is labeled by the genetic marker, because this labeling is neither targeted nor specific (Feng et al., 2000; Badea et al., 2003). The mouse line used by Lin and Masland (2006) showed highly variable reporter expression between transgenic lines that were generated using the same construct (Feng et al., 2000). Therefore, the most complete catalog of cell types must include data from several studies using multiple techniques. At present, 17 types of displaced amacrine cells have been identified in the mouse retina (Table 2; Gustincich et al., 1997; Badea and Nathans, 2004; Lin and Masland, 2006; present study).

Displaced amacrine cells in the mouse compared with other species

Although displaced amacrine cells have been found in almost all vertebrate retinas, the proportions of GCL neurons that are amacrine cells differs from species to species. Displaced amacrine cells make up approximately one-third of the somata in the GCL in rabbit retina (Hughes and Vaney, 1980; Vaney, 1980) and salamander retina (Zhang et al., 2004); 40% in hamster retina (Linden and Esbérard, 1987); 50% in rat retina (Perry and Walker, 1980), guinea pig retina (Kao and Sterling, 2006), and ground squirrel retina (Abreu et al., 1993); and 75–80% in peripheral cat retina (Hughes and Wieniawa-Narkiewicz, 1980; Wässle et al., 1987a) and human retina (Curcio and Allen, 1990). In the mouse retina, displaced amacrine cells make up 59% of the neurons in the GCL (Jeon et al., 1998).

Four cell types identified in this study have been described in other species. The WA-S1 was described by Gallego (1971) and coincides with the type b wide-field unistratified amacrine cell in the rat retina (Perry and Walker, 1980) and the A20 cell in the cat retina (Kolb et al., 1981; Wässle et al., 1987a,b); WA-S1 may be a subtype of the turtle A16 cell (Kolb, 1982). This cell type has a

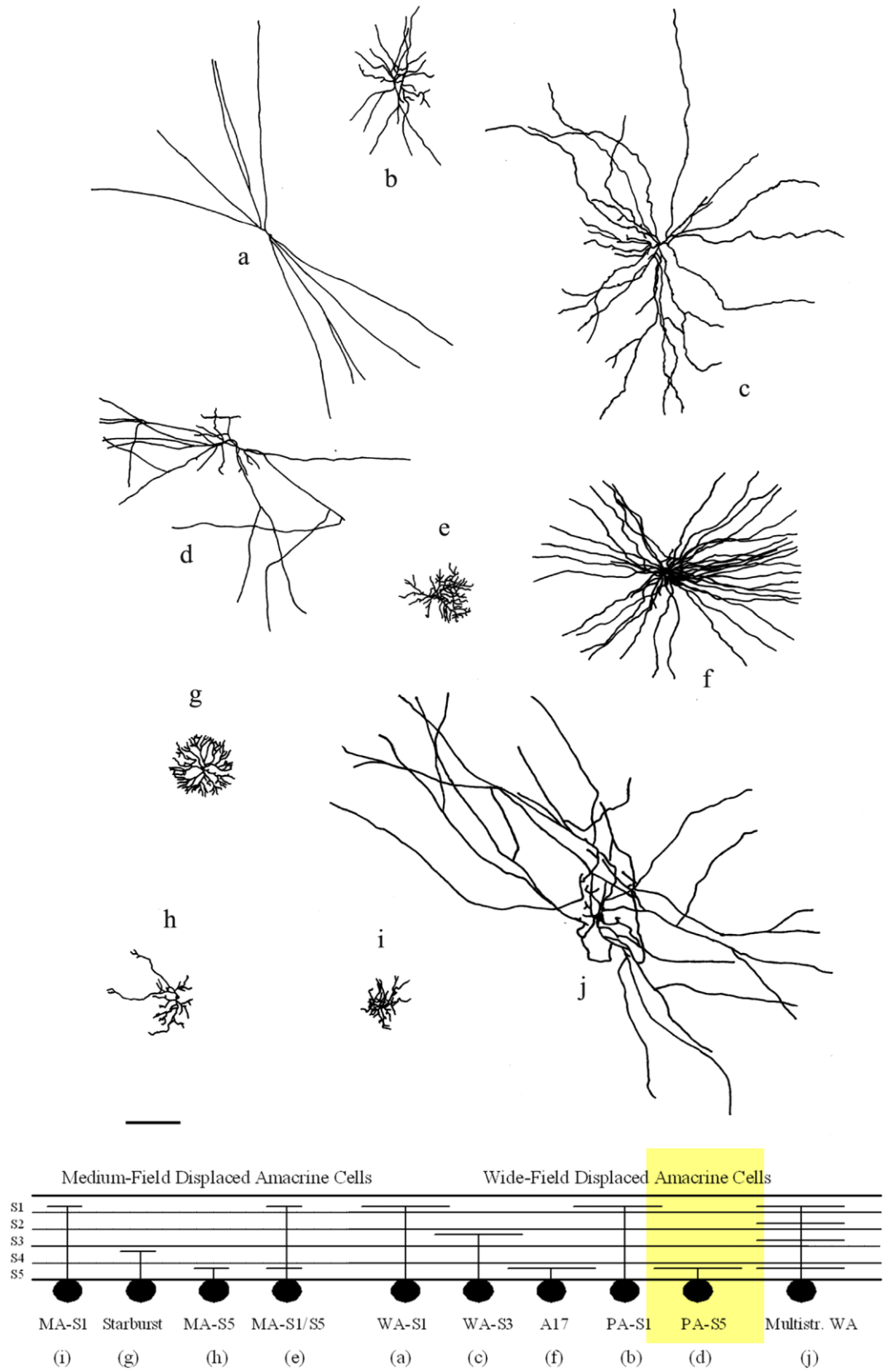

Fig. 6. Illustrations of the 10 displaced amacrine cell types identified in this study. The top panel shows the morphology of each cell type; the bottom panel illustrates the stratification depth of each cell type. Scale bar = 200 μm.

TABLE 2. Overview of the 17 Displaced Amacrine Cell Types Identified to Date in the Mouse Retinas

This study	Badea and Nathans (2004)	Lin and Masland (2006)	Gustincich et al. (1997)
MA-S1			
STARBURST	STARBURST		
MA-S5	CLUSTER 3		
MA-S1/S5			
WA-S1		WA-1	
WA-S3			
A17			
PA-S1			
PA-S5		WA4-1	
MULT. WA			
	A1		
	A1-2		
	CLUSTER 1		
	CLUSTER 4		
	BIFID		
	GIANT AMACRINE		
			TYPE 2 CATECHOLAMINERGIC CELL

counterpart of similar morphology in the INL (rat: Perry and Walker, 1980; rabbit: MacNeil et al., 1999). The WA-S1 stratifies in layer S1 of the IPL (this study; Lin and Masland, 2006), but cells of similar morphology stratify in other layers: a rat homolog stratifies in the inner part of the IPL (Perry and Walker, 1980); the bifid cell stratifies in layer S5 (Badea and Nathans, 2004); and cluster 1 cells stratify in S3 (Badea and Nathans, 2004); we also encountered one such cell stratifying in S3 (not shown). Whether this diversity in stratification reflects functionally distinct cell types is unclear.

The best-characterized displaced amacrine cell is the starburst amacrine cell (for review see Masland and Tauchi, 1986), which makes up 19.5% of the displaced amacrine cells in the mouse retina (Jeon et al., 1998), 55% in the guinea pig retina (Kao and Sterling, 2006), and 85% in the rabbit retina (Vaney et al., 1981). Displaced starburst amacrine cells stratify in layer S4 of the IPL and are mirrored by cells of the same type located in the INL, which ramify in S2. Starburst amacrine cells play an important role in motion detection: they costratify with ON/OFF bistratified ganglion cells (Famiglietti, 1992c; Vaney and Pow, 2000; Zhang et al., 2005) and provide these ganglion cells with direction-selective inhibition (for review see Taylor and Vaney, 2003). This direction selectivity originates in the individual dendritic branches of the starburst cell: each dendrite is selective for stimuli that move along the dendrite away from the soma (Euler et al., 2002). To achieve this direction selectivity, the dendrites of starburst amacrine cells are functionally compartmentalized, whereby differential expression of chloride cotransporters along the length of the dendrite results in corresponding differential effects of GABA on membrane potential (Gavrikov et al., 2006).

The A17 cell was first described in the cat retina by Kolb et al. (1981). This cell type also has a counterpart of identical morphology in the INL (Wässle et al., 1987a). The displaced A17 cell is described here for the first time in the mouse retina. Both displaced and nondisplaced A17 cells stratify in the innermost layer of the IPL (cat: S4 and S5, Nelson and Kolb, 1985; rat: S5, Menger and Wässle, 2000). This GABAergic cell is an important component of the rod pathway: feedback inhibition at the reciprocal rod bipolar/A17 cell synapse shapes light responses in the inner retina (Dong and Hare, 2003), helping to adjust sensitivity levels over a large area of rod photoreceptors (Nelson and Kolb, 1985) and improve the temporal fidelity of light signals in the inner retina (Singer and Diamond, 2003; Dong and Hare, 2003). A17 cells use a unique form of feedback, whereby GABA release is triggered by calcium influx through AMPA receptors, activated by glutamate released from rod bipolar cells (Chavez et al., 2006).

Polyaxonal amacrine cells have also been described previously; this cell class is made up of several physiologically distinct cell types (Völgyi et al., 2001). The PA-S5 cell identified in this study is similar to the PA2 or type III cell found in the rabbit retina (Famiglietti, 1992b; Völgyi et al., 2001). One subtype of polyaxonal amacrine cell is electrically coupled to ON direction-selective ganglion cells; this coupling synchronizes the activity of neighboring ON direction-selective cells and thus plays a role in encoding stimulus movement (Ackert et al., 2006). Polyaxonal amacrine cells may also be involved in inhibition of ganglion cell spiking during rapid global shifts in scenes, such as during eye movements; this inhibition promotes detection of objects moving in a stationary scene (Roska and Werblin, 2003; Ölveczky et al., 2003).

Functional considerations

The presence of displaced amacrine cells in such ancient species as the Australian lungfish (Bailes et al., 2006) suggests a fundamental role for this class of cells. Truly *misplaced* AII amacrine cells have been reported in the outermost part of the INL; these cells are much less common than displaced amacrine cells and probably result from migration errors (Lee et al., 2006). Nevertheless, it is tempting to speculate on the evolutionary advantage of displacing some amacrine cell somata to the GCL. Is there a space problem in the INL? This is unlikely, in that moving all amacrine cells into the INL would add negligibly to the thickness of this layer. Do displaced amacrine cells require a certain proximity to ganglion cell somata? Changes in extracellular potassium concentration at the ganglion cell axon hillocks could influence the membrane potential of nearby displaced amacrine cells, for example, although this is unlikely, because the axon hillock of each ganglion cell is insulated by a continuous sheath from Müller cells (Stone et al., 1995). Whether there is an additional synaptic layer below the GCL has not been clarified (Koontz et al., 1989; Koontz, 1993). Do displaced amacrine cells synapse with ON bipolar cells, whereas nondisplaced amacrine cells contact OFF cells? This mirror-image arrangement, exemplified by the starburst amacrine cells, offers the advantage that the cell body is closer to the synaptic contacts (Wässle et al., 1987a). However, although this organization may be advantageous for some cell types, others stratify in the same layer of the IPL whether their cell bodies are displaced or not. For example, both displaced and nondisplaced A17 cells ramify in layer S5, where they synapse with rod bipolar cells.

This raises the interesting issue of whether some amacrine cells with cell bodies in the GCL may in fact be misplaced. Wright and Vaney (1999) described an amacrine cell type that has 98% of its somata in the INL and 2% displaced to the GCL; these displaced cells seem to be misplaced from the regular array of somata in the INL (Wright and Vaney, 1999). This may also be the case for

A17 cells, which are densely packed in the INL and quite scarce in the GCL. Conversely, some cell types found in the GCL have not been described in the INL (for example, MA-S1 and WA-S3) and therefore seem to be intentionally displaced to the GCL. The OFF starburst amacrine cell is another example of a cell type intentionally displaced to the GCL; this population of cells follows a pattern of development clearly distinct from that of the ON cell population (Knabe et al., 2007).

Several observations suggest that displaced amacrine cells probably have modulatory roles in visual processing. Narrow-field amacrine cells are thought to be involved in the direct pathway of information flow, whereas cells with larger dendritic fields are modulatory, with an indirect influence on information transmission (Masland, 1988); narrow-field amacrine cells are conspicuously absent from the GCL in the mouse (this study), rat (Perry and Walker, 1980), and cat (Wässle et al., 1987a) retinas. Furthermore, the majority of displaced amacrine cells are starburst amacrine cells (this study; Vaney et al., 1981). Thus, although there are many different types of amacrine cell in the GCL, the cells themselves, aside from the starburst cells, are rare, again suggesting a modulatory role in visual processing (see Masland, 1988). Evidence supporting a modulatory role has been provided for polyaxonal amacrine cells, which have been shown to release a number of neurotransmitters, including dopamine (Dacey, 1990) and nitric oxide (Perez et al., 1995).

ACKNOWLEDGMENTS

We thank David Pow for the antibodies against GABA and glycine and Karin Dedek for helpful discussion of the manuscript.

LITERATURE CITED

Aboelela SW, Robinson DW. 2004. Physiological response properties of displaced amacrine cells of the adult ferret retina. Vis Neurosci 21: 135–144.

Abreu M, Kicliter E, Lugo-Garcia N. 1993. Displaced amacrine cells in the ganglion cell layer of the ground squirrel retina. P R Health Sci J 12:137–141.

Ackert JM, Wu SH, Lee JC, Abrams J, Hu EH, Perlman I, Bloomfield SA. 2006. Light-induced changes in spike synchronization between coupled ON direction selective ganglion cells in the mammalian retina. J Neurosci 26:4206–4215.

Badea TC, Nathans J. 2004. Quantitative analysis of neuronal morphologies in the mouse retina visualized by using a genetically directed reporter. J Comp Neurol 480:331–351.

Badea TC, Wang Y, Nathans J. 2003. A noninvasive genetic/pharmacologic strategy for visualizing cell morphology and clonal relationships in the mouse. J Neurosci 23:2314–2322.

Bailes HF, Trezise AEO, Collin SP. 2006. The number, morphology, distribution of retinal ganglion cells and optic axons in the Australian lungfish *Neoceratodus forsteri* (Krefft 1870). Vis Neurosci 23:257–273.

Chavez AE, Singer JH, Diamond JS. 2006. Fast neurotransmitter release triggered by Ca influx through AMPA-type glutamate receptors. Nature 443:705–708.

Curcio CA, Allen KA. 1990. Topography of ganglion cells in human retina. J Comp Neurol 300:5–25.

Dacey DM. 1990. The dopaminergic amacrine cell. J Comp Neurol 301: 461–489.

Dong CJ, Hare WA. 2003. Temporal modulation of scotopic visual signals by A17 amacrine cells in mammalian retina in vivo. J Neurophysiol 89:2159–2166.

Euler T, Detwiler PB, Denk W. 2002. Directionally selective calcium signals in dendrites of starburst amacrine cells. Nature 418:845–852.

Famiglietti EV. 1981. Displaced amacrine cells of the retina. Soc Neurosci Abstr 7:620.

Famiglietti EV. 1992a. Polyaxonal amacrine cells of rabbit retina: morphology and stratification of PA1 cells. J Comp Neurol 316:391–405.

Famiglietti EV. 1992b. Polyaxonal amacrine cells of rabbit retina: PA2, PA3, PA4 cells. Light and electron microscopic studies with a functional interpretation. J Comp Neurol 316:422–446.

Famiglietti EV. 1992c. Dendritic co-stratification of ON and ON-OFF directionally selective ganglion cells with starburst amacrine cells in rabbit retina. J Comp Neurol 324:322–335.

Feng G, Mellor RH, Bernstein M, Keller-Peck C, Nguyen QT, Wallace M, Nerbonne JM, Lichtman, JW, Sanes JR. 2000. Imaging neuronal subsets in transgenic mice expressing multiple spectral variants of GFP. Neuron 28:41–51.

Gallego A. 1971. Horizontal and amacrine cells in the mammal's retina. Vis Res Suppl 3:33–50.

Gavrikov KE, Nilson JE, Dmitriev AV, Zucker CL, Mangel SC. 2006. Dendritic compartmentalization of chloride cotransporters underlies directional responses of starburst amacrine cells in retina. Proc Natl Acad Sci U S A 103:18793–18798.

Gustincich S, Feigenspan A, Wu DK, Koopman LJ, Raviola E. 1997. Control of dopamine release in the retina: a transgenic approach to neural networks. Neuron 18:723–736.

Haverkamp S, Wässle H. 2000. Immunocytochemical analysis of the mouse retina. J Comp Neurol 424:1–23.

Hughes A, Vaney DI. 1980. Coronate cells: the displaced amacrine cells of the rabbit retina? J Comp Neurol 189:169–189.

Hughes A, Wieniawa-Narkiewicz E. 1980. A large, newly identified population of presumptive microneurons in the ganglion cell layer of the cat retina. Nature 284:468–470.

Jeon CJ, Strettoi E, Masland RH. 1998. The major cell populations of the mouse retina. J Neurosci 18:8936–8946.

Kao Y-H, Sterling P. 2003. Matching neural morphology to molecular expression: single cell injection following immunostaining. J Neurocytol 32:245–251.

Kao Y-H, Sterling P. 2006. Displaced GAD65 amacrine cells of the guinea pig retina are morphologically diverse. Vis Neurosci 23:931–939.

Knabe W, Washausen S, Happel N, Kuhn H-J. 2007. Development of starburst cholinergic amacrine cells in the retina of *Tupaia belangeri*. J Comp Neurol 502:584–597.

Kolb H. 1982. The morphology of the bipolar cells, amacrine cells and ganglion cells in the retina of the turtle *Pseudemys scripta elegans*. Philos Trans R Soc Lond B Biol Sci 298:355–393.

Kolb H, Nelson R, Mariani A. 1981. Amacrine cells, bipolar cells and ganglion cells of the cat retina: a Golgi study. Vis Res 21:1081–1114.

Koontz MA. 1993. GABA-immunoreactive profiles provide synaptic input to the soma, axon hillock, and axon initial segment of ganglion cells in primate retina. Vis Res 33:2629–2636.

Koontz MA, Hendrickson AE, Ryan MK. 1989. GABA-immunoreactive synaptic plexus in the nerve fiber layer of primate retina. Vis Neurosci 2:19–25.

Lee EJ, Mann LB, Rickman DW, Lim EJ, Chun MH, Grzywacz NM. 2006. AII amacrine cells in the distal inner nuclear layer of the mouse retina. J Comp Neurol 494:651–662.

Lin B, Masland RH. 2006. Populations of wide-field amacrine cells in the mouse retina. J Comp Neurol 499:797–809.

Linden R, Esbérard CE. 1987. Displaced amacrine cells in the ganglion cell layer of the hamster retina. Vis Res 27:1071–1076.

MacNeil MA, Masland RH. 1998. Extreme diversity among amacrine cells: implications for function. Neuron 20:971–982.

MacNeil MA, Heussy JK, Dacheux RF, Raviola E, Masland RH. 1999. The shapes and numbers of amacrine cells: matching of photofilled with Golgi-stained cells in the rabbit retina and comparison with other mammalian species. J Comp Neurol 413:305–326.

Marc RE, Murry RF, Basinger SF. 1995. Pattern recognition of amino acid signatures in retinal neurons. J Neurosci 15:5106–5129.

Masland RH. 1988. Amacrine cells. TINS 11:405–410.

Masland RH. 2001. The fundamental plan of the retina. Nat Neurosci 4:877–886.

Masland RH, Tauchi M. 1986. The cholinergic amacrine cell. TINS 9:218–223.

Massey SC, Redburn DA. 1987. Transmitter circuits in the vertebrate retina. Prog Neurobiol 28:55–96.

Maxeiner S, Dedek K, Janssen-Bienhold U, Ammermüller J, Brune H, Kirsch T, Pieper M, Degen J, Kruger O, Willecke K, Weiler R. 2005. Deletion of connexin45 in mouse retinal neurons disrupts the rod/cone signaling pathway between AII amacrine and ON cone bipolar cells and leads to impaired visual transmission. J Neurosci 25:566–576.

Menger N, Wässle H. 2000. Morphological and physiological properties of the A17 amacrine cell of the rat retina. Vis Neurosci 17:769–780.

Nelson R, Kolb H. 1985. A17: a broad-field amacrine cell in the rod system of the cat retina. J Neurophysiol 54:592–614.

Ölveczky BP, Baccus SA, Meister M. 2003. Segregation of object and background motion in the retina. Nature 423:401–408.

Perez MT, Larsson B, Alm P, Andersson KE, Ehinger B. 1995. Localisation of neuronal nitric oxide synthase-immunoreactivity in rat and rabbit retinas. Exp Brain Res 104:207–217.

Perry VH, Walker M. 1980. Amacrine cells, displaced amacrine cells and interplexiform cells in the retina of the rat. Proc R Soc Lond B Biol Sci 208:415–431.

Petit-Jacques J, Völgyi B, Rudy B, Bloomfield S. 2005. Spontaneous oscillatory activity of starburst amacrine cells in the mouse retina. J Neurophysiol 94:1770–1780.

Pow DV, Wright LL, Vaney DI. 1995. The immunocytochemical detection of amino-acid neurotransmitters in paraformaldehyde-fixed tissues. J Neurosci Methods 56:115–123.

Roska B, Werblin F. 2003. Rapid global shifts in natural scenes block spiking in specific ganglion cell types. Nat Neurosci 6:600–508.

Sandell JH, Masland RH. 1986. A system of indoleamine-accumulating neurons in the rabbit retina. J Neurosci 6:3331–3347.

Schubert T, Maxeiner S, Krüger O, Willecke K, Weiler R. 2005. Connexin45 mediates gap junctional coupling of bistratified ganglion cells in the mouse retina. J Comp Neurol 490:29–39.

Singer JH, Diamond JS. 2003. Sustained Ca^{2+} entry elicits transient postsynaptic currents at a retinal ribbon synapse. J Neurosci 23: 10923–10933.

Stone J, Makarov F, Hollander H. 1995. The glial ensheathment of the soma and axon hillock of retinal ganglion cells. Vis Neurosci 12:273–279.

Strettoi E, Masland RH. 1996. The number of unidentified amacrine cells in the mammalian retina. Proc Natl Acad Sci U S A 93:14906–14911.

Taylor WR, Vaney DI. 2003. New directions in retinal research. TINS 26:379–385.

Vaney DI. 1980. A quantitative comparison between the ganglion cell populations and axonal outflows of the visual streak and periphery of the rabbit retina. J Comp Neurol 189:215–233.

Vaney DI. 1990. The mosaic of amacrine cells in the mammalian retina. Prog Ret Res 9:49–100.

Vaney DI, Pow DV. 2000. The dendritic architecture of the cholinergic plexus in the rabbit retina: selective labeling by glycine accumulation in the presence of sarcosine. J Comp Neurol 421:1–13.

Vaney DI, Peichl L, Boycott BB. 1981. Matching populations of amacrine cells in the inner nuclear and ganglion cell layers of the rabbit retina. J Comp Neurol 199:373–391.

Völgyi B, Xin D, Amarillo Y, Bloomfield SA. 2001. Morphology and physiology of the polyaxonal amacrine cells in the rabbit retina. J Comp Neurol 440:109–125.

Wässle H, Boycott BB. 1991. Functional architecture of the mammalian retina. Physiol Rev 71:447–480.

Wässle H, Chun MH, Müller F. 1987a. Amacrine cells in the ganglion cell layer of the cat retina. J Comp Neurol 265:391–408.

Wässle H, Voigt T, Patel B. 1987b. Morphological and immunocytochemical identification of indoleamine-accumulating neurons in the cat retina. J Neurosci 7:1574–1585.

Watt CB, Glazebrook PA, Florack VJ. 1994. Localization of substance P and GABA in retinotectal ganglion cells of the larval tiger salamander. Vis Neurosci 11:355–362.

Wright LL, Vaney DI. 1999. The fountain amacrine cells of the rabbit retina. Vis Neurosci 16:1145–1156.

Zhang J, Yang Z, Wu SM. 2004. Immunocytochemical analysis of spatial organization of photoreceptors and amacrine and ganglion cells in the tiger salamander retina. Vis Neurosci 21:157–166.

Zhang J, Li W, Hoshi H, Mills SL, Massey SC. 2005. Stratification of alpha ganglion cells and ON/OFF directionally selective ganglion cells in the rabbit retina. Vis Neurosci 22:535–549.